The Influence of Admixtures to the Signal of an Electromagnetic Flow Meter

Juozapas Arvydas Virbalis, Roma Račkienė * , **Miglė Kriuglaitė-Jarašiūnienė and Konstantinas Otas**

Department of Electrical Power Systems, Faculty of Electrical and Electronics Engineering, Kaunas University of Technology, Studentų str. 48, Kaunas LT-51367, Lithuania; juozapas.virbalis@ktu.lt (J.A.V.); migle.kriuglaite-jarasiuniene@ktu.lt (M.K.-J.); konstantinas.otas@ktu.lt (K.O.)
* Correspondence: roma.rackiene@ktu.lt; Tel.: +370-37-300-267

check for updates

Abstract: Measurement error in an electromagnetic flow meter appears if magnetic and electric properties of admixtures are different from that of the fluid. Expressions of the error, which depends on volume concentration, permeability, and electric conductivity of particles were obtained by approximating the particles' shape as an ellipsoid. Components of the error, which appear inside particles and outside particles in active zone of flow meter, with any canal form are investigated. Expressions of the error are presented assuming that particles are oriented in various directions with respect of the flow direction and are spinning. Different cases of magnetic and electric admixtures properties are discussed. Error expression obtained for flows with nonconductive and nonmagnetic particles coincides with experimental and modelling results obtained by other explorers for flows with air bubbles. Magnetic particles with high electric conductivity are especially dangerous. Extra measurement error in this case greatly depends on the shape of the particle. Measurement error increases if particle shape differs from a sphere. The complementary measurement error can exceed the volume concentration of particles by ten times if the ratio between the longest and the shortest axes of ellipsoid exceeds 3.

Keywords: electromagnetic flow meter; admixtures; measurement error; ellipsoidal particles

1. Introduction

Electromagnetic flow meters (EMFM) for measuring ionic fluid flow in closed completely filled pipes are investigated in this paper. Theoretical foundations of these meters, summarized by J.A. Shercliff [1], lead to the creation of accurate and reliable measuring instruments. Very important impetus to the theory of such gauges was the concept of a virtual current, introduced by M.K. Bevir [2], which allows for accurate estimation of the influence of every flow point over the measurement signal. The ability of assessing the sensitivity to velocity distribution [3], the influence of channel electrical properties on calibration [4,5], including the case when closed pipe is not completely filled [6], and setting of weighting functions has been simplified [7]. The concept of virtual current is also widely used for measuring multiphase flow with EMFM [8]. In the case when the concentration of other phase admixtures is high, other methods are used: electrical resistance tomography [9–11], phase-isolation method [12], or additional electrodes [13].

Further development of multiphase flow measurement theory is hampered by the insufficient analysis regarding how different electric and magnetic properties of admixtures in the flow and particles shape influence the accuracy of EMFM. This article summarizes results of the research carried out by the Kaunas University of Technology.

2. Global and Local Coordinate Systems

In electromagnetic flow meters, the electrode signal is formed by any point of the active zone (the flow volume in which magnetic field acts). We linked the global rectangular coordinate system *xyz* with the active zone. Weight of any active zone point *x*, *y*, *z* over the measurement signal depends on the value of weight vector in this point $\mathbf{W}(x, y, z) = \mathbf{B}(x, y, z) \times \mathbf{J}(x, y, z)$ [2]. In this expression, $\mathbf{B}(x, y, z)$ is the vector of magnetic flux density and $\mathbf{J}(x, y, z)$ is the vector of virtual current density in the point *x*, *y*, *z*. Virtual current density $\mathbf{J}(x, y, z)$ is a formal parameter. It can be calculated as the density of the current equal to 1 A driving from one electrode to the second one when the fluid is at rest [2].

Let us say the fluid flow is parallel to the *z*-axis, i.e., flow velocity has only component v_z, and the *z*-axis coincides with canal axis and the *x*-axis coincides with the line connecting the centers of electrodes and the mean value of velocity equal to $\overline{v} = 1\,\text{m/s}$. It is a normalized regime. Signal *U* can be expressed in this case [14]:

$$\begin{cases} U = \int\limits_{\tau_a} W_z(x, y, z)\mathrm{d}\tau_a; \\ W_z(x, y, z) = J_x(x, y, z)B_y(x, y, z) - J_y(x, y, z)B_x(x, y, z); \end{cases} \tag{1}$$

where τ_a is the volume of the active zone; $W_z(x,y,z)$ is the value of the weight vector *z* component in the point *x*, *y*, *z* of the active zone; and $J_x(x,y,z)$, $B_x(x,y,z)$, $J_y(x,y,z)$, $B_y(x,y,z)$ are the *x* and *y* components of the virtual current **J** and magnetic flux **B** densities vectors at this point.

Considering that the weight vector can be different in any point of the active zone, we express the value of measurement signal U_0 when there are no admixtures in the flow:

$$\begin{cases} U_0 = \left(\dfrac{1}{\tau_a} \int\limits_{\tau_a} W_{z0}\mathrm{d}\tau_a \right) \cdot \tau_a = \overline{W_{z0}}\tau_a; \\ \overline{W_{z0}} = \overline{J_{x0}B_{y0}} - \overline{J_{y0}B_{x0}}; \end{cases} \tag{2}$$

where $J_{x0} = J_{x0}(x,y,z)$, $J_{y0} = J_{y0}(x,y,z)$, $B_{x0} = B_{x0}(x,y,z)$, $B_{y0} = B_{y0}(x,y,z)$ are the values of respective components in the point *x*, *y*, *z* of the active zone without admixtures, $\overline{W_{z0}}$, $\overline{J_{x0}B_{y0}}$, and $\overline{J_{y0}B_{x0}}$ are the mean values of the weight vector *z* component and products of the respective components in all the active zone values when the fluid flow is clean.

Expressions of the measurement signal errors when the fluid is contaminated by small magnetic particles depending on the volume concentration, permeability, and electric conductivity of particles are obtained in Reference [14] for spherical particles and for an ideal electromagnetic flow meter with a rectangular duct and infinitely conductive large electrodes. The real shape of particles is different from a sphere. It is important to investigate dependence of the measurement error on a shape of admixture particles. We approximate particle shape using an ellipsoid. This shape allows for the generalization of particles of very different forms. The limiting cases of ellipsoid are sphere, disc, cylinder, lamella, and other.

Some different particular cases are investigated in References [15,16]. We generalize all cases for ellipsoidal shape of particles and any form of canal.

The shape of admixtures was approximated using an ellipsoid, which can be orientated any way with respect to the global coordinate system. We used a local rectangular coordinate system *q*, *r*, *s*, where axes coincide with axes of the ellipsoid (see Figure 1). The equation of the ellipsoid in this coordinate system is:

$$q^2/a^2 + r^2/b^2 + s^2/c^2 = 1 \tag{3}$$

where *a*, *b*, *c* are the lengths of the ellipsoid semi-axes. We can obtain very different forms of particles by varying ratios a/b and b/c.
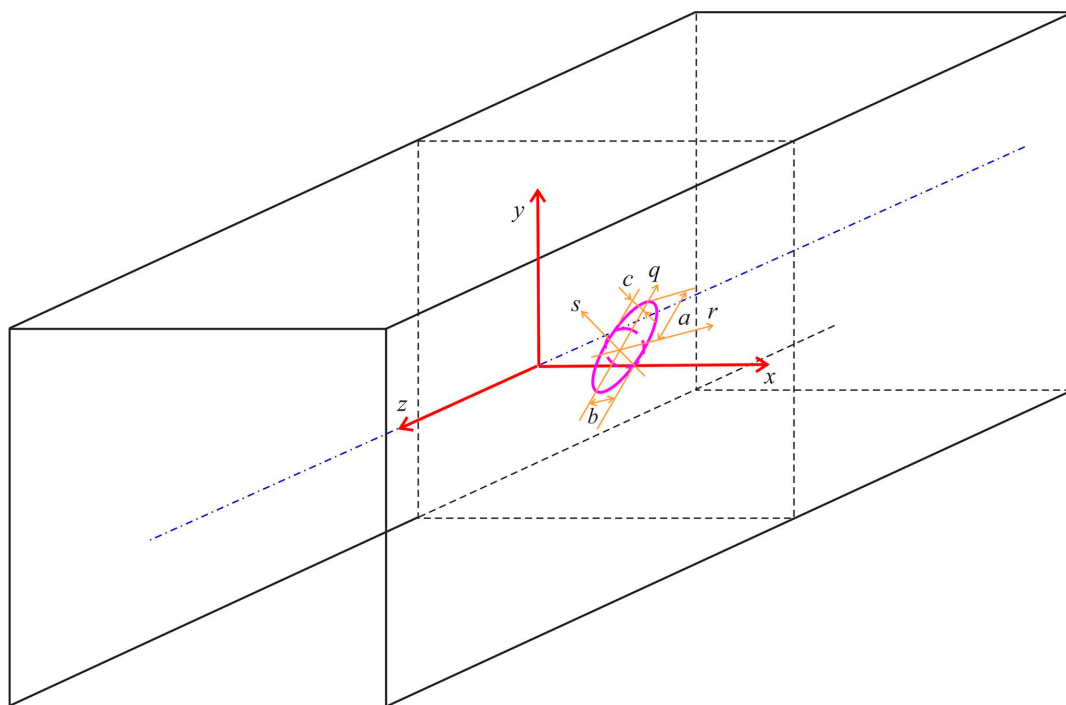
Figure 1. Global and local coordinate systems.

In a rectangular canal of a flow meter with wide electrodes and homogeneous fluid, both magnetic field and virtual current lines are uniform. In a circular channel with spot electrodes, virtual current lines are not uniform, but in an environment of small particles, they may be considered as uniform with a slight error. Therefore, we suppose that irrespective of the meter design, lines of magnetic flux and virtual current densities are distributed uniformly in the volume occupied by the particle before it gets into the flow (see Figure 2a).
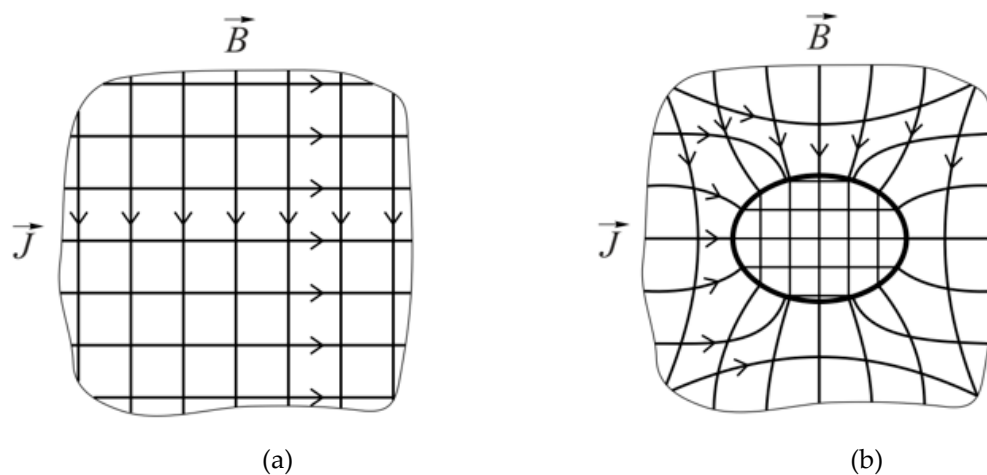

(a)   (b)

Figure 2. Distribution of virtual current $\vec{J}$ and magnetic flux density $\vec{B}$ in the small part of canal cross-section: (**a**) in homogeneous fluid, and (**b**) in the admixture particle and around it.

The distribution of virtual current and magnetic flux density in an ellipsoidal particle with different electrical conductivity and permeability than that of the fluid can be analyzed using an analogy of electrostatic, magnetic field, and electric current.

Let the single admixture particle of volume τ_p get into the active zone of the flow meter. In Figure 2b, it is shown how lines of virtual current and magnetic flux density change if conductive

magnetic ellipsoid enter a rectangular channel. We can see that values of $\vec{J}$ and $\vec{B}$ in comparison with the clean fluid vary inside and outside the particle.

Signal U of the electrodes can be divided into two components:

$$U = U_f\Big|_{\tau=\tau_a-\tau_p} + U_p\Big|_{\tau=\tau_p} = \int\limits_{\tau_a-\tau_p} W_{zf}d\tau + \int\limits_{\tau_p} W_{zp}d\tau \tag{4}$$

Indexes f or p mean that signal U or weight function W are formed in the volume outside or in admixture particle, correspondingly.

To find out the influence of the admixture over the electrode signal, it is necessary to investigate the variation of magnetic flux and virtual current density distributions inside the particle and in the active zone outside the particle.

3. Signal Error inside the Admixture Particle

We suppose that particles are small and distributed evenly in the flow.

The weight function inside the ellipsoidal particle can be calculated this way:

$$W_{zp} = J_{xp}B_{yp} - J_{yp}B_{xp} \tag{5}$$

Using an electric, electric current, and magnetic fields analogy, and using relations obtained in Reference [17], we can relate the components of virtual current and magnetic flux densities inside the particle $J_{xp}, J_{yp}, J_{zp}, B_{xp}, B_{yp}$, and B_{zp} with suitable components in the clean flow $J_{x0}, J_{y0}, J_{z0}, B_{x0}, B_{y0}$, and B_{z0} as follows:

$$\left[J_{xp}, J_{yp}, J_{zp}\right]^T = [h][A^\gamma][h]^T\left[J_{x0}, J_{y0}, J_{z0}\right]^T \tag{6}$$

$$\left[B_{xp}, B_{yp}, B_{zp}\right]^T = [h][A^\mu][h]^T\left[B_{x0}, B_{y0}, B_{z0}\right]^T \tag{7}$$

where:

$$[A^\gamma] = \begin{bmatrix} A_a^\gamma & 0 & 0 \\ 0 & A_b^\gamma & 0 \\ 0 & 0 & A_c^\gamma \end{bmatrix} \tag{8}$$

$$A_a^\gamma = 1 + (C_a - 1)\kappa_a^\gamma, \quad A_b^\gamma = 1 + (C_b - 1)\kappa_b^\gamma, \quad A_c^\gamma = 1 + (C_c - 1)\kappa_c^\gamma \tag{9}$$

$$\kappa_a^\gamma = \frac{1 - \left(\gamma_f/\gamma_p\right)}{1 + (C_a - 1)\left(\gamma_f/\gamma_p\right)}, \quad \kappa_b^\gamma = \frac{1 - \left(\gamma_f/\gamma_p\right)}{1 + (C_b - 1)\left(\gamma_f/\gamma_p\right)}, \quad \kappa_c^\gamma = \frac{1 - \left(\gamma_f/\gamma_p\right)}{1 + (C_c - 1)\left(\gamma_f/\gamma_p\right)} \tag{10}$$

γ_p and γ_f are electrical conductivities of the particles and fluid, correspondingly.

There C_a, C_b, and C_c are the shape factors; $\kappa_a^\gamma, \kappa_b^\gamma$, and κ_c^γ are factors of electric properties, and κ_a^μ, κ_b^μ, and κ_c^μ are factors of magnetic properties.

Factors A^μ can be calculated using Equations (8)–(10) but replacing matrix $[A^\gamma]$ with matrix $[A^\mu]$:

$$[A^\mu] = \begin{bmatrix} A_a^\mu & 0 & 0 \\ 0 & A_b^\mu & 0 \\ 0 & 0 & A_c^\mu \end{bmatrix} \tag{11}$$

$$A_a^\mu = 1 + (C_a - 1)\kappa_a^\mu, \quad A_b^\mu = 1 + (C_b - 1)\kappa_b^\mu, \quad A_c^\mu = 1 + (C_c - 1)\kappa_c^\mu \tag{12}$$

where

$$\kappa_a^\mu = \frac{1 - (1/\mu_p)}{1 + (C_a - 1)(1/\mu_p)}, \quad \kappa_b^\mu = \frac{1 - (1/\mu_p)}{1 + (C_b - 1)(1/\mu_p)}, \quad \kappa_c^\mu = \frac{1 - (1/\mu_p)}{1 + (C_c - 1)(1/\mu_p)} \tag{13}$$

μ_p is the permeability of particles.

Ellipsoid shape factors C_a, C_b, and C_c are Reference [17]:

$$
\begin{cases}
C_a = \dfrac{2}{abc \int\limits_0^\infty dw / \sqrt{(w+a^2)^3 (w+b^2)(w+c^2)}}, \\[2ex]
C_b = \dfrac{2}{abc \int\limits_0^\infty dw / \sqrt{(w+a^2)(w+b^2)^3 (w+c^2)}}, \\[2ex]
C_c = \dfrac{2}{abc \int\limits_0^\infty dw / \sqrt{(w+a^2)(w+b^2)(w+c^2)^3}}.
\end{cases}
\tag{14}
$$

If the local coordinate system is rotated about axis x of a global system by an angle ψ, about axis y by an angle v, and about axis z by an angle ϕ, elements of the matrix $[h]$ have values as follows:

$$
\begin{cases}
h_{11} = \cos v \cos \phi, \\
h_{12} = -\sin \phi \cos v, \\
h_{13} = \sin v, \\
h_{21} = \cos \psi \sin \phi + \sin \psi \sin v \cos \phi, \\
h_{22} = \cos \psi \cos \phi - \sin \psi \sin v \sin \phi, \\
h_{23} = -\sin \psi \cos v, \\
h_{31} = \sin \psi \sin \phi - \cos \psi \sin v \cos \phi, \\
h_{32} = \sin \psi \cos \phi + \cos \psi \sin v \sin \phi, \\
h_{33} = \cos \psi \cos v.
\end{cases}
\tag{15}
$$

Equations (5)–(14) are obtained for the case when the longest semi-axis a coincides with the q-axis, the semi-axis of the mean length b coincides with the r-axis, and the shortest semi-axis c coincides with the s-axis of the local coordinate system.

In reality, particles can take any position with respect to the global coordinate system. Besides, mostly they rotate intensely in the stream. Therefore, in Equation (5) average values of virtual current and magnetic flux density must be estimated correspondingly $\overline{J_{px}}$, $\overline{J_{py}}$ and $\overline{B_{py}}$, $\overline{B_{px}}$ for any position of the particle. First, the case is analyzed when the local coordinate system axes are rotated, respectively at angles ψ, v, and ϕ with respect to the axes of the global system, but ellipsoidal semi-axes a, b, and c can be oriented in direction of any axis of the local system. Let us denote semi-axes directed in the q direction as i, semi-axes directed in s direction as j, and semi-axes directed in r direction as k. From Table 1, it can be seen that there are six different possible combinations of the local system axes and ellipsoidal semi-axes. In this case, instead of matrices $[A^\gamma]$ and $[A^\mu]$, matrices $\left[A^\gamma_{ijk}\right]$ and $\left[A^\mu_{ijk}\right]$ are used:

$$
\left[A^\gamma_{ijk}\right] = \begin{bmatrix} A^\gamma_i & 0 & 0 \\ 0 & A^\gamma_j & 0 \\ 0 & 0 & A^\gamma_k \end{bmatrix}, \quad
\left[A^\mu_{ijk}\right] = \begin{bmatrix} A^\mu_i & 0 & 0 \\ 0 & A^\mu_j & 0 \\ 0 & 0 & A^\mu_k \end{bmatrix}
\tag{16}
$$

Table 1. Possible orientations of ellipsoid semi-axes with respect to the local system axes.

	Semi-axes		
N	i	j	k
1	a	b	c
2	b	c	a
3	c	a	b
4	a	c	b
5	b	a	c
6	c	b	a

In Equations (6) and (7), using $\left[A_{ijk}^{\gamma}\right]$ and $\left[A_{ijk}^{\mu}\right]$ instead of $[A^{\gamma}]$ and $[A^{\mu}]$, and appreciating that $J_{z0} = B_{z0} = 0$, we can express, respectively, J_{xp}, J_{yp} and B_{yp}, B_{xp} as:

$$J_{xp} = \left(h_{11}^2 A_i^{\gamma} + h_{12}^2 A_j^{\gamma} + h_{13}^2 A_k^{\gamma}\right) J_{x0} + \left(h_{11}h_{21}A_i^{\gamma} + h_{12}h_{22}A_j^{\gamma} + h_{13}h_{23}A_k^{\gamma}\right) J_{y0} \tag{17}$$

$$J_{yp} = \left(h_{11}h_{21}A_i^{\gamma} + h_{12}h_{22}A_j^{\gamma} + h_{13}h_{23}A_k^{\gamma}\right) J_{x0} + \left(h_{21}^2 A_i^{\gamma} + h_{22}^2 A_j^{\gamma} + h_{23}^2 A_k^{\gamma}\right) J_{y0} \tag{18}$$

$$B_{xp} = \left(h_{11}^2 A_i^{\mu} + h_{12}^2 A_j^{\mu} + h_{13}^2 A_k^{\mu}\right) B_{x0} + \left(h_{11}h_{21}A_i^{\mu} + h_{12}h_{22}A_j^{\mu} + h_{13}h_{23}A_k^{\mu}\right) B_{y0} \tag{19}$$

$$B_{yp} = \left(h_{11}h_{21}A_i^{\mu} + h_{12}h_{22}A_j^{\mu} + h_{13}h_{23}A_k^{\mu}\right) B_{x0} + \left(h_{21}^2 A_i^{\mu} + h_{22}^2 A_j^{\mu} + h_{23}^2 A_k^{\mu}\right) B_{y0} \tag{20}$$

The weight function of the electromagnetic flow meter signal is a vector product of vectors *B* and *J*. Components of multiplication of collinear vectors are equal to zero. Therefore, the expression of the weight function inside the ellipsoidal particle we get by using Equations (17)–(20) for Equation (5), and eliminating of expression after multiplication the components with $J_{x0}B_{x0}$ and $J_{y0}B_{y0}$, is as follows:

$$\begin{aligned}W_{zp} = &\left[h_{12}h_{21}(h_{12}h_{21} - h_{11}h_{22})A_j^{\gamma}A_i^{\mu} + h_{11}h_{22}(h_{11}h_{22} - h_{21}h_{12})A_i^{\gamma}A_j^{\mu} + h_{13}h_{21}(h_{13}h_{21} - h_{11}h_{23})A_k^{\gamma}A_i^{\mu}\right.\\ &\left.+h_{13}h_{22}(h_{13}h_{22} - h_{12}h_{23})A_k^{\gamma}A_j^{\mu} + h_{11}h_{23}(h_{11}h_{23} - h_{21}h_{13})A_i^{\gamma}A_k^{\mu} + h_{12}h_{23}(h_{12}h_{23} - h_{13}h_{22})A_j^{\gamma}A_k^{\mu}\right] J_{x0}B_{y0}\\ &-\left[h_{12}h_{21}(h_{12}h_{21} - h_{11}h_{22})A_j^{\mu}A_i^{\gamma} + h_{11}h_{22}(h_{11}h_{22} - h_{21}h_{12})A_i^{\mu}A_j^{\gamma} + h_{13}h_{21}(h_{13}h_{21} - h_{11}h_{23})A_k^{\mu}A_i^{\gamma}\right.\\ &\left.+h_{13}h_{22}(h_{13}h_{22} - h_{12}h_{23})A_k^{\mu}A_j^{\gamma} + h_{11}h_{23}(h_{11}h_{23} - h_{21}h_{13})A_i^{\mu}A_k^{\gamma} + h_{12}h_{23}(h_{12}h_{23} - h_{13}h_{22})A_j^{\mu}A_k^{\gamma}\right] J_{y0}B_{x0}.\end{aligned} \tag{21}$$

Any value of i, j, and k in Equation (21) are likely with the same probability, therefore in order to calculate the average value $\overline{W_{zp}}$ in Equation (21), we replace any of products $A_{ijk}^{\gamma} \cdot A_{ijk}^{\mu}$ by the average $\overline{A^{\gamma}A^{\mu}}$, which is:

$$\overline{A^{\gamma}A^{\mu}} = 1/6\left(A_a^{\gamma}A_b^{\mu} + A_a^{\gamma}A_c^{\mu} + A_b^{\gamma}A_a^{\mu} + A_b^{\gamma}A_c^{\mu} + A_c^{\gamma}A_a^{\mu} + A_c^{\gamma}A_b^{\mu}\right) \tag{22}$$

Then, the average of weight function $\overline{W_{zp}}$ is as follows:

$$\overline{W_{zp}} = \overline{A^{\gamma}A^{\mu}} \cdot \overline{H(\varphi, \nu, \psi)} \cdot \overline{W_{z0}} \tag{23}$$

where

$$\begin{aligned}\overline{H(\phi, \nu, \psi)} = &\left[h_{11}{}^2\left(h_{22}{}^2 + h_{23}{}^2\right) + h_{12}{}^2\left(h_{21}{}^2 + h_{23}{}^2\right) + h_{13}{}^2\left(h_{21}{}^2 + h_{22}{}^2\right)\right]\\ &-2(h_{11}h_{22}h_{12}h_{21} + h_{11}h_{23}h_{13}h_{21} + h_{12}h_{23}h_{13}h_{22}).\end{aligned} \tag{24}$$

Please note that the $\overline{W_{zp}}$ expression is only a partial average when the local coordinate system is rotated with respect to the global system, respectively, by angles ψ, ν, and ϕ. As these angles can take any number, the global average $\overline{\overline{W_{zp}}}$ may be obtained by entering $\overline{\overline{H}}$ to Equation (23), where $\overline{\overline{H}}$ is the mean value of $\overline{H(\phi, \nu, \psi)}$ when angles ϕ, ν, ψ vary in the range $[0, \pi/2]$. Evaluating Equation (24) after integration, we have: $\overline{\overline{H}} = \frac{8}{\pi^3} \int_0^{\pi/2} \int_0^{\pi/2} \int_0^{\pi/2} \overline{H(\phi, \nu, \psi)} \mathrm{d}\psi \mathrm{d}\phi \mathrm{d}\nu = 1$.

The mean weight function value in the spinning ellipsoidal particle using Equation (23) is:

$$\overline{\overline{W_{zp}}} = \overline{\overline{H}} \cdot \overline{A^{\gamma}A^{\mu}} \cdot \overline{W_{z0}} = \overline{A^{\gamma}A^{\mu}} \cdot \overline{W_{z0}} \tag{25}$$

For the spinning particle, we can express the component of error δ_p caused by signal variation inside the spinning particle using Equations (1), (3), (5), and (22) as follows:

$$\delta_p = \frac{(\overline{U}_p - U_0)\tau_p}{U_0 \cdot \tau_a} = \left(\frac{\overline{U}_p}{U_0} - 1\right) \cdot k = \left(\frac{\overline{\overline{W_{zp}}}}{\overline{W_{z0}}} - 1\right) \cdot k = \left(\overline{A^{\gamma}A^{\mu}} - 1\right) \cdot k \tag{26}$$

where $\overline{U_p}$ is the average value of the signal inside the admixture particle, τ_p is the volume of the particle, and:

$$k = \tau_p / \tau_a \tag{27}$$

is the volume concentration of admixtures.

We express the error component δ_p via shape, electric, and magnetic properties factors using Equations (9), (12), and (22) as follows:

$$
\begin{aligned}
\delta_p = \tfrac{1}{6} k \Big\{ & 2 \Big[(C_a - 1)\left(\kappa_a^\gamma + \kappa_a^\mu \right) + (C_b - 1)\left(\kappa_b^\gamma + \kappa_b^\mu \right) + (C_c - 1)\left(\kappa_c^\gamma + \kappa_c^\mu \right) \Big] \\
& + (C_a - 1)(C_b - 1)\left(\kappa_a^\gamma \kappa_b^\mu + \kappa_b^\gamma \kappa_a^\mu \right) + (C_a - 1)(C_c - 1)\left(\kappa_a^\gamma \kappa_c^\mu + \kappa_c^\gamma \kappa_a^\mu \right) \\
& + (C_b - 1)(C_c - 1)\left(\kappa_b^\gamma \kappa_c^\mu + \kappa_c^\gamma \kappa_b^\mu \right) \Big\}.
\end{aligned}
\tag{28}
$$

As Equations (26)–(28) are the same for any ellipsoidal particle, they can be generalized for all admixture particles. In this case τ_p is the volume of all admixture particles.

4. Error Due to Virtual Current and Magnetic Field Distortion

When a particle with volume τ_p and different from fluid physical properties gets into the active zone, it distorts the magnetic field and virtual current in the residual active zone volume $\tau_a - \tau_p$. We can write the variation of the electrode signal ΔU_d due to this distortion:

$$\Delta U_d = \int\limits_{\tau_a - \tau_p} \overline{\Delta W_{zf}}\, d\tau, \quad \overline{\Delta W_{zf}} = \overline{W_{zf}} - \overline{W_{z0}} \tag{29}$$

where $\overline{W_{z0}}$ and $\overline{W_{zf}}$ are mean values of the weight vector z component at any point of volume outside particle $\tau_a - \tau_p$ in the clean fluid and in the fluid with admixtures, correspondingly.

For the ΔU_d investigation, we use the local ellipsoidal coordinate system ξ, η, ζ [17]. A link to this system with the local rectangular coordinate system q, r, s is shown in Figure 3.
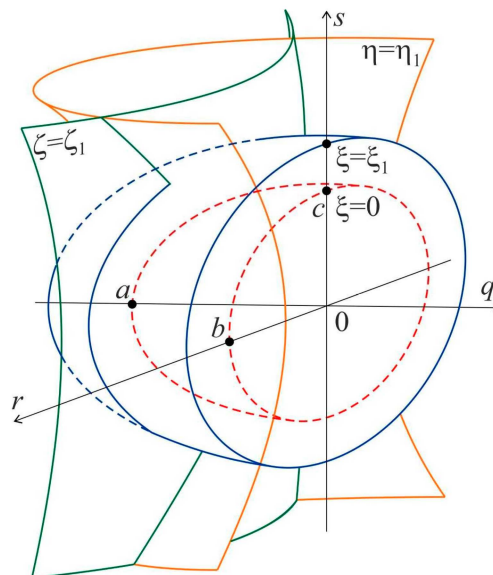
Figure 3. Rectangular q, r, s and ellipsoidal ξ, η, ζ local coordinate systems.

The equation of ellipsoidal particle surface in the ellipsoidal coordinate system is $\xi = 0$. To calculate function $\overline{\Delta W_{zf}(\xi, \eta, \zeta)}$, we use Green's theorem written as follows:

$$\int\limits_{\tau - \tau_p} grad\beta grad\gamma \, d\tau = \oint\limits_S \beta(grad\gamma dS) - \int\limits_{\tau - \tau_p} \beta divgrad\gamma \, d\tau \qquad (30)$$

Let us note that $grad\gamma = \mathbf{e}_\xi \overline{\Delta W_{zf}(\xi, \eta, \zeta)}$ and $\beta = \int h_\xi d\xi$ (h_ξ is the Lame coefficient of coordinate ξ in ellipsoidal coordinate system). Then $\frac{\partial \beta}{\partial \xi} = h_\xi$ and $grad\beta = \mathbf{e}_\xi \frac{1}{h_\xi} \frac{\partial \beta}{\partial \xi} = \mathbf{e}_\xi$. Surface S in the second integral of Equation (30) is composed of the surfaces $\xi = 0$ and $\xi = \xi_L > 0$. There are no sources of $\mathbf{J}$ and $\mathbf{B}$ in the volume $\tau_a - \tau_p$ and $divgrad\gamma = div\left[\mathbf{e}_\xi \overline{\Delta W_{zf}(\xi, \eta, \zeta)}\right] = 0$. Therefore, the Equation (30) expresses the electrode signal variation ΔU_d because of virtual current and magnetic field distortion:

$$\Delta U_d = \int\limits_{\tau_a - \tau_p} \overline{\Delta W_{zf}(\xi, \eta, \zeta)} \, d\tau = \oint\limits_S \left[\int h_\xi d\xi\right] \overline{\Delta W_{zf}(\xi, \eta, \zeta)} \, dS = I_{\xi=0} + I_{\xi=\xi_L} \qquad (31)$$

where $I_{\xi=0}$ and $I_{\xi=\xi_L}$ are the values of the surface integral on the particle surface and on the $\xi_L = $ const, correspondingly.

Let us investigate a particle with $\gamma_p \to \infty$ and $\mu_p \to \infty$. On the surface $\xi = 0$ of such a particle, the equality $\overline{W_{z\infty}} = (\mathbf{J} \times \mathbf{B})_z = 0$ is valid because vectors $\mathbf{J}$ and $\mathbf{B}$ are perpendicular to the surface at any point. Therefore, their directions coincide and vector product $[\mathbf{J} \times \mathbf{B}]$ is equal to zero. This equality is independent of the particle position with respect to the global coordinate system.

By this equality, we can express mean value of the variation $\overline{\Delta W_{z\infty}}(0)$ of the weight vector z component on the surface of particle with $\gamma_p \to \infty$ and $\mu_p \to \infty$:

$$\overline{\Delta W_{z\infty}}(0) = \overline{W_{z\infty}} - \overline{W_{z0}} = -\overline{W_{z0}} = -\left(\overline{J_{x0}B_{y0}} - \overline{J_{y0}B_{x0}}\right) \qquad (32)$$

In this case we can write integral $I_{\xi=0}$ as follows:

$$I_{\xi=0} = \int\limits_{S_{\xi=0}} \left[\int h_\xi d\xi\right]_{\xi=0} \cdot \overline{\Delta W_{z\infty}}(0) \cdot h_\eta h_\zeta d\eta d\zeta = -\overline{\Delta W_{z0}} \cdot \int\limits_{-b^2}^{-c^2} \int\limits_{-a^2}^{-b^2} \left[\int h_\xi d\xi\right]_{\xi=0} h_\eta h_\zeta d\eta d\zeta = -\overline{\Delta W_{z0}} \cdot \tau_p \qquad (33)$$

With an increase of coordinate $\xi_L > 0$, the shape of ellipsoid $\xi = \xi_L$ is nearer to the shape of a sphere with radius $R = \sqrt{\xi + a^2}$ (see Reference [17]) and integral $I_{\xi=\xi_L}$ can be expressed in spherical coordinates. With an increase of R, I_{ξ_L} drops to zero very quickly: $I_{\xi_L} = (-W_0 \tau_p)(a^3/R^3) \to 0$. Therefore, outside the particle with $\gamma_p \to \infty$ and $\mu_p \to \infty$, the signal variation using Equations (31) and (33) is:

$$\Delta U_{d\infty} = -\overline{W_{z0}} \cdot \tau_p \qquad (34)$$

In Reference [14], there were relations obtained between the variation mean values of the virtual current density $\overline{\Delta J_p}$ and $\overline{\Delta J_{p\infty}}$, and magnetic flux density $\overline{\Delta B_p}$ and $\overline{\Delta B_{p\infty}}$ in the real particles and in the particles with $\gamma_p \to \infty$ and $\mu_p \to \infty$, correspondingly, for a spherical shape. We can use the obtained equations for ellipsoidal particles in this way:

$$\overline{\Delta J_p} = \overline{\kappa^\gamma} \cdot \overline{\Delta J_{p\infty}}, \; \overline{\Delta B_p} = \overline{\kappa^\mu} \cdot \overline{\Delta B_{p\infty}} \qquad (35)$$

For spinning particles, $\overline{\kappa^\gamma}$ and $\overline{\kappa^\mu}$ are:

$$\overline{\kappa^\gamma} = \left(\kappa_a^\gamma + \kappa_b^\gamma + \kappa_c^\gamma\right)/3, \; \overline{\kappa^\mu} = \left(\kappa_a^\mu + \kappa_b^\mu + \kappa_c^\mu\right)/3 \qquad (36)$$

The variation of weight vector *z* component using Equation (33) in the common case is:

$$\overline{\Delta W_z} = \overline{\Delta J_x\, \Delta B_y} - \overline{\Delta J_y\, \Delta B_x} = \overline{\kappa^\gamma} \cdot \overline{\kappa^\mu} \cdot \left(\overline{\Delta J_{x\infty}\Delta B_{y\infty}} - \overline{\Delta J_{y\infty}\Delta B_{x\infty}} \right) = -\overline{\kappa^\gamma} \cdot \overline{\kappa^\mu} \cdot \overline{W_0} \tag{37}$$

The mean value of the product $\overline{\kappa^\gamma \kappa^\mu}$ was obtained by multiplying $\overline{\kappa^\gamma}$ by $\overline{\kappa^\mu}$ from Equation (30). As factors $\overline{\kappa^\gamma}$ and $\overline{\kappa^\mu}$ are related by being perpendicular to each other in components $\overline{\Delta J_{x(y)}}$ and $\overline{\Delta B_{y(x)}}$, we can only multiply factors $\kappa^\gamma_{a,b,c}$ and $\kappa^\mu_{a,b,c}$ related with different ellipsoid axes. As a result, we have:

$$\overline{\kappa^\gamma \kappa^\mu} = 1/6 \left(\kappa^\gamma_a \kappa^\mu_b + \kappa^\gamma_a \kappa^\mu_c + \kappa^\gamma_b \kappa^\mu_a + \kappa^\gamma_b \kappa^\mu_c + \kappa^\gamma_c \kappa^\mu_a + \kappa^\gamma_c \kappa^\mu_b \right) \tag{38}$$

In the common case, the mean value of the signal variation $\overline{\Delta U_d}$ because of virtual current and magnetic flux distortion is:

$$\overline{\Delta U_d} = -\overline{\kappa^\gamma} \cdot \overline{\kappa^\mu} \cdot \overline{W_{z0}} \cdot \tau_p \tag{39}$$

The error component δ_d due to the virtual current and magnetic flux distortion outside particles is:

$$\delta_d = \frac{\overline{\Delta U_d}}{\int\limits_{\tau_a - \tau_b} W_{z0}\, d\tau} = -\overline{\kappa^\gamma} \cdot \overline{\kappa^\mu} \cdot \frac{\overline{W_{z0}} \cdot \tau_p}{\overline{W_{z0}} \cdot (\tau_a - \tau_p)} \approx -\overline{\kappa^\gamma} \cdot \overline{\kappa^\mu} \cdot k \tag{40}$$

For all possible values of $\overline{\kappa^\gamma}$ and $\overline{\kappa^\mu}$, the value of δ_d lays in the interval $[0, -k]$.

5. Error Due to Magnetic Flux Density Variation

If magnetic particles get into active zone of the EMFM mean value of permeability of all active zone μ_m varies. This expression of μ_m was obtained for spherical magnetic particles in Reference [14] by analogy with the expression in Reference [17] for the mean value of electrical permittivity of the dilute suspension of spherical particles:

$$\mu_m = 1 + \frac{\tau_p}{\tau_a} A^\mu_s \left(1 - \frac{1}{\mu_p} \right) \tag{41}$$

where $A^\mu_s = \frac{B_p}{B_0}$, and B_0, and B_p are the values of magnetic flux densities, correspondingly, in clean fluid without particles and inside magnetic particle.

The influence of a spinning non-spherical particle to the mean value $\overline{B_{ym}}$ of an external magnetic field is the same as the influence of spherical particle but factor A^μ_s for ellipsoidal particle must be exchanged with the mean value of factor $\overline{A^\mu}$. In the case of an ellipsoidal particle, factor $\overline{A^\mu}$ can be expressed by noting that magnetic flux density mean value variation has no influence on virtual current:

$$\overline{A^\mu} = 1/3 \left(A^\mu_a + A^\mu_b + A^\mu_c \right) \tag{42}$$

The mean value of the *y* component of magnetic flux density $\overline{B_{ym}}$ in all volume τ_a (including volume τ_p of particles) when magnetic particles get into the active zone is:

$$\overline{B_{ym}} = \mu_m \overline{B_{y0}} = \left[1 + \overline{A^\mu} \left(1 - \frac{1}{\mu_p} \right) \frac{\tau_p}{\tau_a} \right] \cdot \overline{B_{y0}} \tag{43}$$

Noting that the mean value of magnetic flux density in the fluid volume $\tau_a - \tau_p$ outside particles is $\overline{B_{yf}}$, we can express the $\overline{B_{ym}}$ another way:

$$\overline{B_{ym}} = \overline{B_{yf}} \cdot \frac{\tau_a - \tau_p}{\tau_a} + \overline{A^\mu}\, \overline{B_{y0}} \cdot \frac{\tau_p}{\tau_a} \tag{44}$$

Comparing Equations (43) and (44), we obtain the expression for the mean value of the increment of magnetic flux density in volume $\tau_a - \tau_p$, i.e., outside particle, $\overline{\Delta B_{yf}}$:

$$\overline{\Delta B_{yf}} = \overline{B_{yf}} - \overline{B_{y0}} = \left(1 - \frac{\overline{A^\mu}}{\mu_p}\right) \cdot \frac{\tau_p}{\tau_a - \tau_p} \cdot \overline{B_{y0}} \tag{45}$$

For spinning particles, the increment $\overline{\Delta B_{xf}}$ is expressed via analogy to $\overline{\Delta B_{yf}}$:

$$\overline{\Delta B_{xf}} = \overline{B_{xf}} - \overline{B_{x0}} = \left(1 - \frac{\overline{A^\mu}}{\mu_p}\right) \cdot \frac{\tau_p}{\tau_a - \tau_p} \cdot \overline{B_{x0}} \tag{46}$$

The mean variation value of signal $\overline{\Delta U_B}$ in the active zone outside particle due to an increment of the mean value of magnetic flux density, supposing that virtual current is not varied, and evaluating Equations (45) and (46) is:

$$\overline{\Delta U_B} = \int\limits_{\tau_a - \tau_p} \overline{\Delta W_z} \, d\tau = \int\limits_{\tau_a - \tau_p} \overline{\left(J_{x0}\Delta B_{yf} - J_{y0}\Delta B_{xf}\right)} \, d\tau = \overline{W_{z0}} \left(1 - \frac{\overline{A^\mu}}{\mu_p}\right) \cdot \frac{\tau_p}{\tau_a - \tau_p} \cdot \int\limits_{\tau_a - \tau_p} d\tau = \overline{W_{z0}}\left(1 - \frac{\overline{A^\mu}}{\mu_p}\right) \cdot \tau_p \tag{47}$$

We can obtain from Equation (13):

$$1 - \frac{1}{\mu_p} = \kappa_a^\mu + \frac{1}{\mu_p} \cdot \kappa_a^\mu \cdot (C_a - 1) \tag{48}$$

After transformation and evaluating Equation (12) we have:

$$1 - \frac{1}{\mu_p} \cdot \left[1 + \kappa_a^\mu \cdot (C_a - 1)\right] = 1 - \frac{A_a^\mu}{\mu_p} = \kappa_a^\mu \tag{49}$$

By analogy, we obtain

$$1 - \frac{A_b^\mu}{\mu_p} = \kappa_b^\mu \tag{50}$$

$$1 - \frac{A_c^\mu}{\mu_p} = \kappa_c^\mu \tag{51}$$

After summing the left and right sides of Equations (49)–(51), dividing both sides by 3, and evaluating Equation (44), we have:

$$1 - \frac{\overline{A^\mu}}{\mu_p} = \frac{1}{3}\left(\kappa_a^\mu + \kappa_b^\mu + \kappa_c^\mu\right) = \overline{\kappa}^\mu \tag{52}$$

Using Equation (52) with Equation (47), we can express relative error δ_B due to variation ΔU_B analogically to δ_p:

$$\delta_B = \frac{\Delta U_B}{\int\limits_{\tau_a - \tau_p} \overline{W_{z0}} \, d\tau} = \frac{\overline{W_{z0}} \cdot \overline{\kappa}^\mu \cdot \tau_p}{\overline{W_{z0}} \cdot (\tau_a - \tau_p)} = \overline{\kappa}^\mu \cdot \frac{k}{1 - k} \approx \overline{\kappa}^\mu \cdot k \tag{53}$$

6. Error Due to the Virtual Current Variation

Using the concept of a virtual current [2], we obtain the distribution of its density if electrodes of flowmeter are connected to a source of 1 A. Therefore, mean values of virtual current density components $\overline{J_x}$ and $\overline{J_y}$ cannot vary in cross-sections perpendicular to the axes x and y, correspondingly.

Variation of the mean value of virtual current density inside the particle may be expressed as:

$$\overline{\Delta J_{xp}} = \overline{J_{xp}} - \overline{\Delta J_{x0}} = \left(\overline{A^\gamma} - 1\right)\overline{J_{x0}} \tag{54}$$

For spinning particles, we must calculate $\overline{A^\gamma}$ as a mean value analogically to Equation (36) for $\overline{A^\mu}$. We express the summands using Equation (9):

$$\overline{A^\gamma} = \left(A_a^\gamma + A_b^\gamma + A_c^\gamma\right)/3 = 1 + \left[(C_a - 1)\kappa_a^\gamma + (C_b - 1)\kappa_b^\gamma + (C_c - 1)\kappa_c^\gamma\right]/3 \tag{55}$$

Variation of $\overline{\Delta J_{xp}}$ in volume τ_p is the reason for the variation of the mean value of component $\overline{\Delta J_{xf}}$ in the fluid outside the particle but in volume τ_a–τ_p and with a contrary sign. Therefore:

$$\overline{\Delta J_{xf}} = -\overline{\Delta J_{xp}}\frac{\tau_p}{\tau_a - \tau_p} \tag{56}$$

The relative variation of the mean value of virtual current density x component in the volume of active zone outside of particles τ_a–τ_p: $\delta_J = \overline{\Delta J_{xf}}/\overline{J_{x0}}$. For spinning particles, values $\overline{J_{y0}}$ and $\overline{\Delta J_{yf}}$ can be related to the same equation as $\overline{J_{x0}}$ and $\overline{\Delta J_{xf}}$: $\left|\overline{\Delta J_{yf}}\right| = \delta_J\left|\overline{J_{y0}}\right|$. Evaluating these relations, we can express mean value of variation of the z component of the weight vector $\overline{\Delta W_J}$ due to variation of virtual current density outside particle is:

$$\overline{\Delta W_J} = \overline{\Delta J_x B_{y0} - \Delta J_y B_{x0}} = \delta_J \cdot \overline{\left(J_{x0}B_{y0} - J_{y0}B_{x0}\right)} = \delta_J \overline{W_0} \tag{57}$$

By integrating both sides of this equation in volume τ_a–τ_p, we obtain the electrode signal variation due to the virtual current density mean value variation outside particles $\overline{\Delta U_J}$:

$$\overline{\Delta U_J} = \int_{\tau_a - \tau_p} \overline{\Delta W_J}\,\mathrm{d}\tau = \int_{\tau_a - \tau_p} \delta_J \overline{W_0}\,\mathrm{d}\tau = \delta_J \overline{U_0} \tag{58}$$

Therefore, δ_J represents a relative error caused by virtual current variation outside particle. It can be expressed using Equations (54) and (56):

$$\delta_J = \frac{\Delta J_{xf}}{J_{x0}} = -\frac{\Delta J_{xp}}{J_{x0}} \cdot \frac{\tau_p}{\tau_a - \tau_p} = -\left(\overline{A^\gamma} - 1\right)\frac{k}{1-k} \approx -\left(\overline{A^\gamma} - 1\right)k \tag{59}$$

Substituting Equation (55) into Equation (59), we express the partial error that appears due to variation of the mean value of virtual current outside particles as follows:

$$\delta_J = -1/3\left[(C_a - 1)\kappa_a^\gamma + (C_b - 1)\kappa_b^\gamma + (C_c - 1)\kappa_c^\gamma\right]k \tag{60}$$

7. Common Expression of Error and Expressions for Partial Cases

The common value of the error δ when the flow has some admixtures is equal to the sum of expressions of partial errors Equations (26), (40), (53), and (60). It can be expressed as:

$$
\begin{aligned}
\delta = \delta_p + \delta_d + \delta_B + \delta_J = \tfrac{1}{6}\Big\{ & C_a C_b\left(\kappa_a^\gamma \kappa_b^\mu + \kappa_b^\gamma \kappa_a^\mu\right) + C_b C_c\left(\kappa_b^\gamma \kappa_c^\mu + \kappa_c^\gamma \kappa_b^\mu\right) + C_c C_a\left(\kappa_c^\gamma \kappa_a^\mu + \kappa_a^\mu \kappa_c^\gamma\right) \\
& - C_a\left[\kappa_a^\gamma\left(\kappa_b^\mu + \kappa_c^\mu\right) + \kappa_a^\mu\left(\kappa_b^\gamma + \kappa_c^\gamma - 2\right)\right] - C_b\left[\kappa_b^\gamma\left(\kappa_c^\mu + \kappa_a^\mu\right) + \kappa_b^\mu\left(\kappa_c^\gamma + \kappa_a^\gamma - 2\right)\right] \\
& - C_c\left[\kappa_c^\gamma\left(\kappa_a^\mu + \kappa_b^\mu\right) + \kappa_c^\mu\left(\kappa_a^\gamma + \kappa_b^\gamma - 2\right)\right] \Big\} \cdot k.
\end{aligned}
\tag{61}
$$

Expression of maximum error value δ_m: Maximum value of error δ_m will be in the case if $\gamma_p \to \infty$, $\mu_p \to \infty$. We can write $\kappa_a^\gamma = \kappa_b^\gamma = \kappa_c^\gamma = \kappa_a^\mu = \kappa_b^\mu = \kappa_c^\mu = 1$ in this case, and δ_m can be expressed this way:

$$\delta_m = 1/3\left[C_a(C_b - 1) + C_b(C_c - 1) + C_c(C_a - 1)\right]k \tag{62}$$

For spherical particles $C_a = C_b = C_c = 3$ and $\delta_m = 6$. An analogous result was obtained in Reference [14] for a rectangular duct.

Expression of common error δ_1, if electrical conductivity of magnetic particles is close to conductivity of fluid: If electrical conductivity of magnetic particles with $\mu_p \gg 1$ is comparable with electrical conductivity of fluid $\gamma_p \cong \gamma_f$, we obtain: $\kappa_a^\gamma \approx \kappa_b^\gamma \approx \kappa_c^\gamma \approx 0$. The value of the error δ_1 in this case is:

$$\delta_1 = (1/3) \cdot \left(C_a \overline{\kappa_a^\mu} + C_b \overline{\kappa_b^\mu} + C_c \overline{\kappa_c^\mu} \right) \tag{63}$$

For spherical particles, δ_1 is in the interval $[0, k]$. It reaches the maximum value for magnetic particles.

Expression of error δ_n for nonconductive magnetic particles: These equations are correct for nonconductive $\gamma_p \ll \gamma_f$ magnetic particles with $\mu_p \gg 1$: $\kappa_a^\gamma = -1/(C_a - 1)$, $\kappa_b^\gamma = -1/(C_b - 1)$, $\kappa_c^\gamma = -1/(C_c - 1)$, and $A_a^\gamma = A_b^\gamma = A_c^\gamma = 0$. Value of the error in this case δ_n is:

$$\delta_n = \frac{1}{3}\left(3 + \frac{1}{C_a - 1} + \frac{1}{C_b - 1} + \frac{1}{C_c - 1} \right) k \tag{64}$$

Value of error δ_{nm} when admixtures are non-magnetic ($\mu_p = 1$): We note the common error for non-magnetic particles by δ_{nm}. These equations are correct for the following case: $A_a^\mu = A_b^\mu = A_c^\mu = 1$, $\delta_d = 0$, $\delta_p = \left[\frac{1}{3}\left(A_a^\gamma + A_b^\gamma + A_c^\gamma \right) - 1 \right] \cdot k$, $\delta_B = 0$, and $\delta_J = -\left[\frac{1}{3}\left(A_a^\gamma + A_b^\gamma + A_c^\gamma \right) - 1 \right] \cdot \frac{k}{1-k}$. We obtain, after summation:

$$\delta_{nm} = -\left[\frac{1}{3}\left(A_a^\gamma + A_b^\gamma + A_c^\gamma \right) - 1 \right] \cdot \frac{k^2}{1-k} \approx -\left[\frac{1}{3}\left(A_a^\gamma + A_b^\gamma + A_c^\gamma \right) - 1 \right] \cdot k^2 \tag{65}$$

In case of non-conducting, for example, gaseous admixtures, we have $A_a^\gamma = A_b^\gamma = A_c^\gamma = 0$ and $\delta_{nm} = -k^2/(1-k)$. In Reference [18], Bernier and Brennen obtained electrode signal of electromagnetic flow meter $U_a = U_0/(1-k)$ for flow with a concentration of air bubbles k, where the U_0 signal for the same fluid flow Q_0 without air. As the total flow of suspension is $Q_0(1+k)$, the signal must be $U_0(1+k)$.

Therefore, the suspension is measured with error $\delta_{BB} = U_0\left(1 + k - \frac{1}{1-k}\right)/U_0 = -\frac{k^2}{1-k}$. This result coincides with the result obtained in this paper: $\delta_{BB} = \delta_{nm}$. Analogical results are obtained in References [19,20] too.

The measurement error for non-conducting or spherical non-magnetic particles has appreciable value when the volume concentration of particles exceeds 5%. The measurement uncertainty for conductive and elongate particles can be appreciable in case of lower particle concentration. For particles with high conductivity, Equation (59) will be $\delta_{nm}|_{\gamma_p \to \infty} \approx -\left[\frac{1}{3}(C_a + C_b + C_c) - 1 \right] \cdot k^2$.

8. Modelling

We calculated range of meter transfer coefficients $\overline{\overline{K_{F\text{maxmax}}}}$ and $\overline{\overline{K_{Fn\text{max}}}}$ variation in the case of very conductive and nonconductive magnetic particles, correspondingly, using program package MATLAB (7.0.1, MathWorks, Natick, MA, USA). The values C_a, C_b, C_c were calculated using Equation (6) and the values of factors $\overline{\overline{K_{F\text{maxmax}}}}$ and $\overline{\overline{K_{Fn\text{max}}}}$ using Equation (19), when $c > b > a$ and ratios $e = b/a$ and $g = c/b$ were varied in the intervals [0.1, 0.95] with the step size of 0.05. Results are presented in Figures 4 and 5.

It can be seen that shape of the particle had a small influence on the measurement error of magnetic particles when the particles were not conductive. The maximum possible measurement error was determined practically using particle volume concentration in this case.

When particles were conductive, the shape of the particle had a great impact on the measurement error.
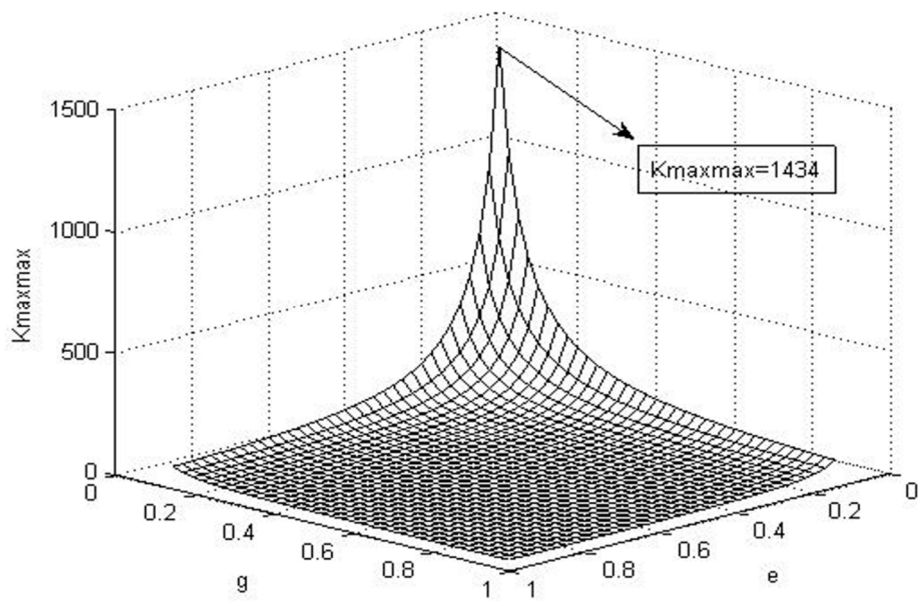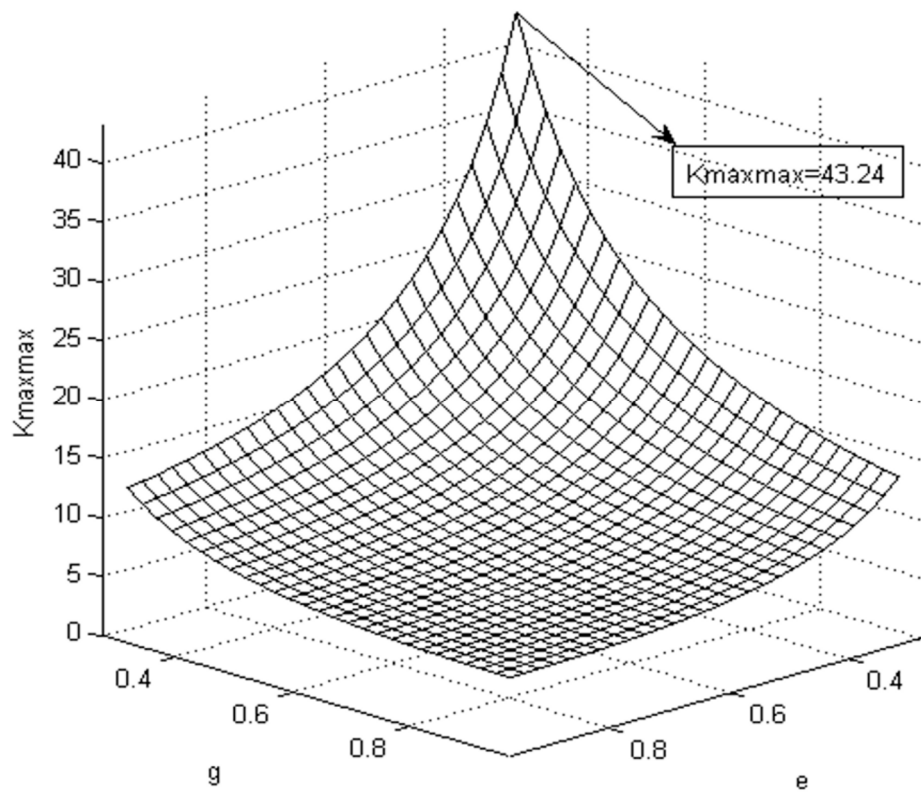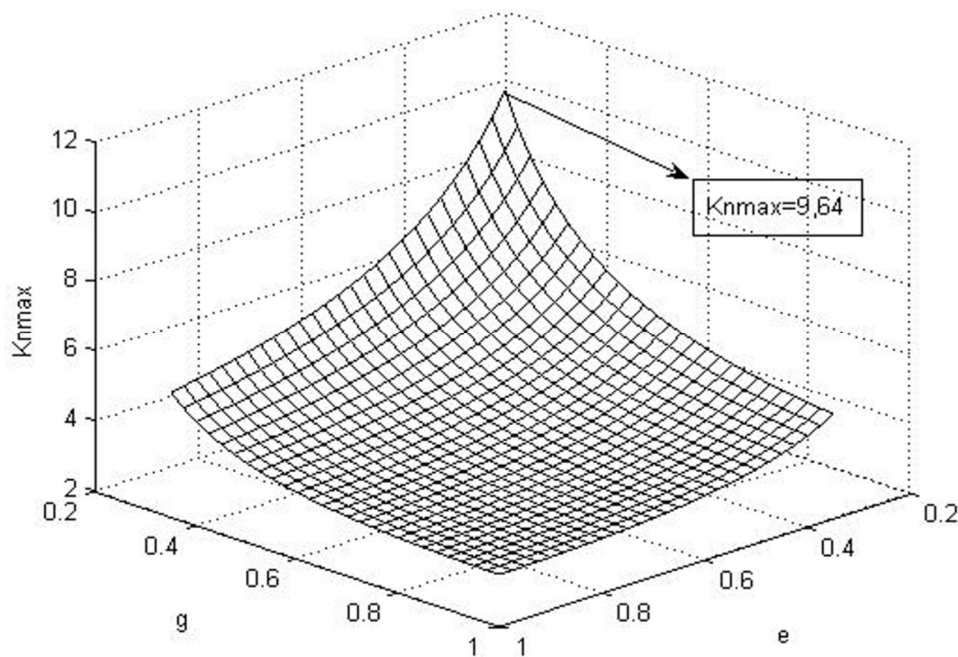
(**a**)
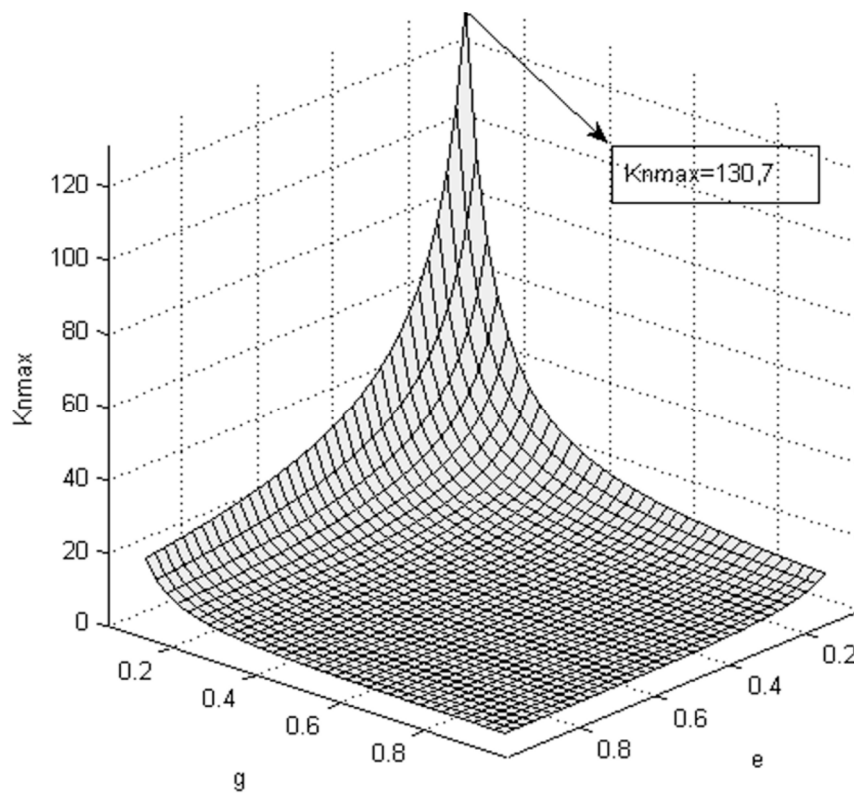
(**b**)

Figure 4. Dependence of factors $\overline{\overline{K_{F\mathrm{maxmax}}}}$ (**a**) and $\overline{\overline{K_{Fn\mathrm{max}}}}$ (**b**) on *g* and *e*, when the interval of *g* and *e* variation was [0.1; 0.95].

(a)

(b)

Figure 5. Dependence of factors $\overline{\overline{K_{F\text{maxmax}}}}$ (**a**) and $\overline{\overline{K_{Fn\text{max}}}}$ (**b**) on *g* and *e*, when the interval of *g* and *e* variation was [0.3; 0.95].

Measurement error for non-magnetic admixture particles was proportional to the second power of relative volume concentration k^2, but it can be valuable for a small concentration in the case of very elongated particles. For example, let us say metallic non-magnetic particle, whose shape is

a rectangular parallelepiped $0.1 \times 1 \times 10 \text{ mm}^3$, is in an active fluid volume of an electromagnetic flow meter. This particle can be approximated as an ellipsoid with ratios of semi axes: $e = b/a = 10$ and $g = c/b = 10$. The value of factor $\overline{\overline{K_{Fn\max}}}$ was equal to 130.7 (see Figure 5). Extra measurement error was equal to 1% if the relative volume concentration was equal to 0.87% in this case. Very elongated and very conductive magnetic particles with $\gamma_p >> \gamma_m$ and $\mu_p >> 1$ were especially dangerous. We obtained from Figure 5 that for very conductive magnetic particles with dimensions $0.1 \times 1 \times 10 \text{ mm}^3$, $\overline{\overline{K_{Fmaxmax}}} \approx 1434$ and $\delta_{maxmax} \approx 1434\, k$. Let this particle get into an active zone of electromagnetic flow meter with a rectangular $30 \times 20 \text{ mm}^2$ channel and plain electrodes with width $l = 10$ mm. The active fluid volume, in which the main part of electrode signal was formed, was evaluated as $\tau_a \approx 30 \times 20 \times 10 = 6000 \text{ mm}^3$. The particle volume was 1 mm^3 and volume concentration was $k \approx 1/6000 \approx 1.67 \times 10^{-4}$. Therefore, in the time interval when the particle flows in the active fluid volume, the extra measurement error was $\delta_{maxmax} \approx 24\%$.

9. Discussion and Conclusions

Analysis made in this paper allows for the reliable assessment of the error of an electromagnetic flow meter with admixtures in EMFM, depending on particles' shape, and electric and magnetic properties, if concentration of admixtures in the fluid does not exceed 5–10%. By approximating particles as ellipsoids, a variety of different particle forms may be evaluated. Admixtures may be solid, liquid, or gaseous. Analysis was made with the assumption that fluid flow was turbulent and particles of admixtures were spinning. The maximum error was caused by long and narrow magnetic particles with higher electrical conductivity than of the fluid. If the ratio between length and width a/b was also a ratio between width and height b/c that exceeded 10, error may exceed the relative concentration of particles k up to 1000 times. Cases like this are almost impossible in turbulent flow, as long and narrow particles break up in such a flow. However, if the concentration of magnetic conductive particles is sufficient, the error is not less than $6k$. The latter value was obtained for spherical particles. If the ratio between the longest and the shortest axis of particle cross-section did not exceed 3, the error was $\delta_{maxmax} \approx (11–12)\cdot k$. Therefore, if the concentration of such particles is high enough, the accuracy of measurement significantly drops.

In case of laminar flow because of very long particles error should not increase highly as oblong particles orientate along the flow.

Conclusions reached in the analysis were verified using MATLAB software. Verification of the results done by other authors [18–20], both in measuring and modeling flows with air bubbles, are especially valuable.

Recently, special attention is paid to the application of electromagnetic flow meters for measuring flows of several phases [8–13]. Results of this analysis may be successfully applied there too.

In the near future, the authors are going to verify results using finite elements method using ANSYS and to verify the model with existing experimental results obtained in the standardized test rigs for EMFM calibration. Also, the authors will focus on applying analyzed methods for multiphase flows with significant concentration of different phases.

Author Contributions: J.A.V. supervised the research and mathematical implementation, and was responsible for methods development and summarizing the results. All the authors contributed in literature review. R.R. performed analysis of the signal error inside the admixture particle and the error due to the virtual current and magnetic field distortion, M.K.-J. performed analysis of the error due to the magnetic flux density variation and because of the virtual current variation, and K.O. formulated the common expression of error and expressions for partial cases. All the authors performed the results analysis, discussion, modelling part, and contributed to writing the paper.

References

1. Shercliff, J.A. *Electromagnetic Flow Measurement*; Cambridge University Press: Cambridge, UK, 1962.

2. Bevir, M.K. The theory of induced voltage electromagnetic flowmeters. *J. Fluid Mech.* **1970**, *43*, 577–590. [CrossRef]
3. Hemp, J.; Wyatt, D.G. A basis for comparing the sensitivities of different electromagnetic flowmeters to velocity distribution. *J. Fluid Mech.* **1981**, *112*, 189–201. [CrossRef]
4. Wang, J.Z.; Tian, G.Y.; Lucas, G.P. Relationship between velocity profile and distribution of induced potential for an electromagnetic flow meter. *Flow Meas. Instrum.* **2007**, *18*, 99–105. [CrossRef]
5. Baker, R.C. On the concept of Virtual Current as a Means to Enhance Verification of Electromagnetic Flowmeters. *Meas. Sci. Technol.* **2011**, *22*, 105403. [CrossRef]
6. Zhang, X.-Z. The virtual current of an electromagnetic flow meter in partially filled pipes Flowmeters. *Meas. Sci. Technol.* **1998**, *9*, 1852–1855. [CrossRef]
7. Wang, J.Z.; Lucas, G.P.; Tian, G.Y. A numerical approach to the determination of electromagnetic flow meter weight functions. *Meas. Sci. Technol.* **2007**, *18*, 548–554. [CrossRef]
8. Zhang, X.-Z. 2D analysis for the virtual current distribution in an electromagnetic flow meter with a bubble at various axis positions. *Meas. Sci. Technol.* **1998**, *9*, 1501–1515. [CrossRef]
9. Deng, X.; Li, G.; Wei, Z.; Yan, Z.; Yang, W. Theoretical Study of Vertical Slug Flow Measurement by Data Fusion from Electromagnetic Flowmeter and Electrical Resistance Tomography meter. *Flow Meas. Instrum.* **2011**, *22*, 272–278. [CrossRef]
10. Meng, Y.; Lucas, G.P. Imaging Water Velocity and Volume Fraction Distributions in Water Continuous Multiphase Flows Using Inductive Flow Tomography and Electric Resistance Tomography. *Meas. Sci. Technol.* **2017**, *28*, 055401. [CrossRef]
11. Muhamedsalih, Y.; Lucas, G.P.; Meng, Y.P. A Two-phase flow meter for determining water and solids volumetric flow rates in stratified, inclined solids-in-water flows. *Flow Meas. Instrum.* **2015**, *45*, 207–217. [CrossRef]
12. Yang, Y.; Wang, D.; Niu, P.; Liu, M.; Wang, S. Gas-liquid two-Phase flow measurements by the electromagnetic flowmeter combined with a phase-isolation method. *Flow Meas. Instrum.* **2018**, *60*, 78–87. [CrossRef]
13. Leeungculsatien, T.; Lucas, G.P. Measurement of velocity profiles in Multi-Electrode Electromagnetic Flow Meter. *Flow Meas. Instrum.* **2013**, *21*, 86–95. [CrossRef]
14. Virbalis, J.A. Errors in electromagnetic flow meter with magnetic particles. *Flow Meas. Instrum.* **2001**, *12*, 275–282. [CrossRef]
15. Šimeliūnas, R.; Virbalis, J.A. Investigation of field of ellipsoidal shape magnetic particle. *Electron. Electr. Eng.* **2002**, *42*, 72–77.
16. Pakenas, V.; Virbalis, J.A. Influence of non-magnetic admixtures to the signal of electromagnetic flow meter. *Electron. Electr. Eng.* **2011**, *116*, 7–11. [CrossRef]
17. Landau, L.D.; Lifshitz, E.M. *Electrodynamics of Continuous Media*; Nauka: Moskow, Russia, 1982; 620p.
18. Bernier, R.N.; Brennen, C.E. Use of the electromagnetic flowmeter in a two-phase flow. *Int. J. Multiph. Flow* **1983**, *9*, 251–257. [CrossRef]
19. Cha, J.-E.; Ahn, Y.-C.; Kim, M.-H. Flow measurement in an electromagnetic flowmeter in two-phase bubbly and slug flow regimes. *Flow Meas. Instrum.* **2002**, *12*, 329–339. [CrossRef]
20. Opara, U.; Bajslae, J. Concurrent two-phase downflow measurement with an induced voltage electromagnetic flowmeter. *J. Hydraul. Res.* **2001**, *39*, 93–98. [CrossRef]